UDC 539.4

Static and Dynamic Tearing of Thin Steel Sheets

M. Aberkane,[a] A. Ouibrahim,[b] G. Pluvinage,[a] and Z. Azari[a]

[a] Laboratoire de Fiabilité Mécanique, Université de Metz, France

[b] Laboratoire d'Energétique Mécanique et Matériaux, Université de Boumerdes, Algeria

УДК 539.4

Статические и динамические испытания тонколистовой стали на сдвиг

М. Аберкан[а], А. Уибрахим[б], Г. Плювинаж[а], З. Азари[а]

[а] Университет г. Мец, Франция

[б] Университет г. Бумэрди, Алжир

Представлен энергетический анализ статического разрушения тонких стальных листов по типу K_{III}. При динамических испытаниях использовалось оборудование для образцов типа Шарпи. Статические испытания трех видов стальных листов на разрыв свидетельствуют, что линейное соотношение Мая–Коттрелла справедливо для образцов с шириной рабочей части до 30 мм. В указанном диапазоне удельная работа разрушения Γ_e определяется в соответствии с моделью Мая–Коттрелла. Исследовалась кинетика Γ_e в зависимости от толщины листа B, радиуса кривизны ρ и скорости нагружения V. Усовершенствованная модель включает линейное отношение ρ/W. Кроме того, изменение скорости нагружения V от 1 до 300 мм/мин показало, что удельная работа разрушения Γ_e не зависит от нее. Установлено незначительное снижение динамической трещиностойкости $J_{0,d}$.

Ключевые слова: вязкое разрушение, образцы для испытаний на разрыв по типу K_{III}, работа разрушения, установка для испытания образцов типа Шарпи.

Notation

A – elongation
a – crack length
a_{ph} – distance between the root and the leg free edge
B – specimen thickness
b – ligament length
b_{ph} – distance of plastic hinge travel
dU_e – elementary elastic strain work
dU_p – elementary total nonessential work of fracture
dU_1 – elementary plastic bending work
dU_2 – elementary plastic unbending work
dx – elementary length of the legs
E – Young's modulus

$IC_{95\%}$ – confidence interval at 95%
J – J-integral
J_0 – toughness at crack initiation
$J_{0,d}$ – dynamic toughness at crack initiation
$K_{Ic,st}$ – static mode I stress intensity factor
$K_{Ic,d}$ – dynamic mode I stress intensity factor
L – middle leg length
L_{ph} – length of the middle leg after the second stage
M_e – elastic moment
M_p – plastic moment
M_{p1} – plastic bending moment
M_{p2} – limit plastic bending moment
m – striking mass of the middle leg
n – work hardening exponent
R_e – yield strength
R_m – ultimate strength
R_0 – flow stress
$R_{0,d}$ – dynamic flow stress
r_1 – mode III toughness ratio
r_2 – mode I toughness ratio
P – external force
SD – standard deviation
T – tearing modulus
T_d – dynamic tearing modulus
u – displacement of the load application point
U – work spent on fracture
v_i – initial velocity of the hook
v_f – final velocity of the hook
V – loading rate
W – leg width
α, β – constants
ε – total strain
ε_e – elastic component of the total strain
ε_p – plastic component of the total strain
Γ_e – essential work of fracture
ρ – radius of curvature
ρ_e – elastic radius of curvature
ρ_0 – plastic radius of curvature
σ – stress
σ_0 – stress value per unit strain
η – η-factor
θ_p – total plastic angle
θ_{ph1} – middle leg rotation at the “built-in” end (root)
θ_{ph2} – angle of the root at the plastic hinge
Δ – relative error
ΔW_R – change of rotational energy

Introduction. The toughness of some extremely ductile materials such as swaging steels cannot be described with the classical fracture mechanics criteria such as the critical stress intensity factor or the critical value of the J-integral. For thin sheets in particular, Cotterell and Reddel [1] have developed the initial idea of Broberg [2] who stated that two regions are necessarily found around the crack tip. The first one is the fracture process region and the second one, which surrounds the first region, is called the screening region [3]. The total work of fracture is composed of the work required in the crack process region and the work spent in the screening region [4]. The work in the first region is called "essential work of fracture" and is mainly concerned with crack propagation. Mai and Cotterell [5] performed two-leg and three-leg trouser tests for tearing of ductile sheet materials, where gross plasticity is developed following crack propagation. For the analysis, they assumed that the work of plastic bending and unbending of the legs during the tearing process is described by the mean radius of curvature ρ. With the use of an incremental rigid plastic energy balance to describe the process, their solution for the tearing force is simply a symmetrical two-legged trouser tear, assuming that the behavior of the sheet material is governed by the stress-strain relationship of a power law type. They show a linear behavior between the force per unit thickness and the tab width. The specific essential work of fracture Γ_e is determined by extrapolation of the linear curve.

In the present work, we investigate tearing of thin steel sheets in mode III considering a theoretical approach as well as experimental tests.

Thus,

a) The Mai–Cotterell analysis [5] is extended to take into account the elastic contribution to the energy balance by adding the work spent during elastic deformation.

b) Tests are conducted for studying the effect of the width exceeding 30 mm, the radius of curvature, and thickness on the specific essential work of fracture.

c) The influence of the loading rate V on Γ_e (calculated from Mai–Cotterell analysis [5]) is considered for the values of V between 1 and 300 mm/min.

d) Moreover, dynamic tearing tests ($V = 3 \cdot 10^5$ mm/min) of thin sheet steel are performed. A new original experimental method is proposed and a comparison is made between the values of the specific essential work and the dynamic fracture toughness at initiation.

Static Tearing Tests.

Theoretical Analysis. The trousers tearing tests determine the essential work of fracture Γ_e for thin metal sheets in mode III tearing. Mai and Cotterell [5] considered only the energy balance in tearing of thin metal sheets. If the legs of a specimen are large enough, the elastic as well as the plastic strain work induced in the legs is negligible. Thus, the work of the external force P is mainly spent on breaking the specimen. Hence, the energy balance is expressed by the following relation:

$$Pdu = \Gamma_e B da, \tag{1}$$

where B is the specimen thickness, u is the displacement of the load application point, a is the initial value of the crack length (Fig. 1a), and Γ_e is the essential work of fracture.

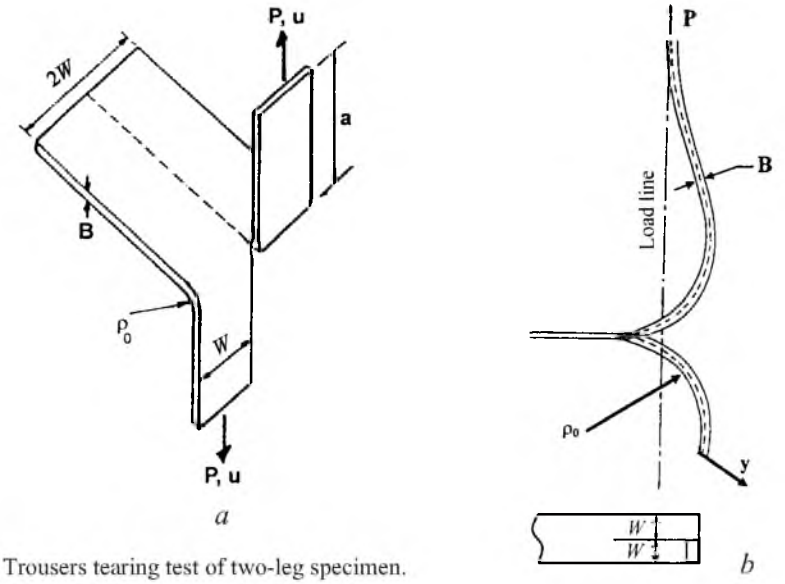

Fig. 1. Trousers tearing test of two-leg specimen.

Geometrical considerations lead to the equation $u = 2a$. Then Eq. (1) gives

$$\Gamma_e = \frac{2P}{B}. \tag{2}$$

If the specimen legs are not large enough, the elastic and plastic strain work in the legs must be taken into account in the energy balance. The energy balance, in this case, is expressed by

$$Pdx = \frac{\Gamma_e B dx}{2} + dU_p, \tag{3}$$

where dU_p is the total nonessential work necessary to bend and unbend the length dx of the legs.

The curvature $1/\rho$ of the leg is the sum of the elastic curvature corresponding to the yield stress R_e, the curvature $1/\rho_e$, and the plastic curvature during bending of the leg with the curvature of $1/\rho_0$. The total strain ε is equal to

$$\varepsilon = \varepsilon_e + \varepsilon_p. \tag{4}$$

Here ε_e and ε_p are the elastic and plastic components of the total strain, respectively.

$$\varepsilon = \frac{y}{\rho} = y\left(\frac{1}{\rho_e} + \frac{1}{\rho_0}\right), \tag{5}$$

where y is the distance between the neutral axis and the outer fiber (Fig. 1b), while the elastic curvature $1/\rho_e$ is given by

$$\frac{1}{\rho_e} = \frac{2R_e}{BE}. \tag{6}$$

Here R_e is the yield strength and E is the Young modulus. We considered the elastic moment defined by

$$M_e = 2W \int_0^{B/2} \left(\frac{y}{\rho_e}\right) Eydy = \frac{WEB^3}{12\rho_e}, \tag{7}$$

where W is the specimen leg width (Fig. 1a). The elementary elastic work is equal to

$$dU_e = dx \int_0^{\rho_e} M_e d\left(\frac{1}{\rho}\right) = \frac{WBR_e^2}{6E} dx. \tag{8}$$

In the plastic field, the material behaves following the power law:

$$\sigma = \sigma_0 \varepsilon^n, \tag{9}$$

where σ_0 and n are the stress value of the unit strain and the work hardening exponent, respectively.

Figure 1b represents a specimen after ductile tearing. The plastic bending moment is given by

$$M_{p1} = 2W \int_0^{B/2} \sigma y dy. \tag{10}$$

Combination of Eqs. (5), (9), and (10) leads to

$$M_{p1} = \frac{\sigma_0 B^{n+2} W}{\rho^n (n+2) 2^{n+1}}. \tag{11}$$

The elementary plastic work dU_1 required to bend the length dx of the leg is given by

$$dU_1 = dx \int_{1/\rho_e}^{1/\rho_e + 1/\rho_0} M_{p1} d\left(\frac{1}{\rho}\right). \tag{12}$$

Upon integration, Eq. (12) takes the following form:

$$dU_1 = \frac{\sigma_0 B^{n+2} W}{2^{n+1}(n+1)(n+2)} \left[\left(\frac{1}{\rho_e} + \frac{1}{\rho_0}\right)^{n+1} - \left(\frac{1}{\rho_e}\right)^{n+1}\right] dx. \tag{13}$$

When the plastic moment given by Eq. (11) reaches its limit, the specimen leg develops plastic unbending. With respect to relation (11), the limit moment M_{p2} is equal to

$$M_{p2} = \frac{\sigma_0 B^{n+2} W}{(n+2)2^{n+1}} \left[\frac{1}{\rho_0} + \frac{1}{\rho} \right], \tag{14}$$

where ρ is the radius of curvature during unbending. The elementary plastic work dU_2 required for unbending of the element dx of the specimen leg is given by

$$dU_2 = dx \int_{1/\rho_e}^{1/\rho_0} M_{p2} d\left(\frac{1}{\rho}\right). \tag{15}$$

By using (14) and integrating (15), we arrive at the following equation:

$$dU_2 = \frac{\sigma_0 B^{n+2} W}{2^{n+1}(n+1)(n+2)} \left[\left(\frac{2}{\rho_0}\right)^{n+1} - \left(\frac{1}{\rho_e} + \frac{1}{\rho_0}\right)^{n+1} \right] dx. \tag{16}$$

The total elementary nonessential plastic work dU_p is the sum of (13) and (16), and is defined by the following relation:

$$dU_p = dU_1 + dU_2 = \frac{\sigma_0 B^{n+2} W}{2^{n+1}(n+1)(n+2)} \left[\left(\frac{2}{\rho_0}\right)^{n+1} - \left(\frac{1}{\rho_e}\right)^{n+1} \right] dx, \tag{17a}$$

$$dU_p = dU_1 + dU_2 = \frac{\sigma_0 B^{n+2} W}{2^{n+1}(n+1)(n+2)} \left(\frac{1}{\rho_0}\right)^{n+1} \left[1 - \left(\frac{\rho_0}{2\rho_e}\right)^{n+1} \right] dx. \tag{17b}$$

Relation (17a) describes the contributions of the plastic and the elastic strain energies per unit length. The relative contribution of the plastic strain energy to the elastic one is given by the ratio $(\rho_0/2\rho_e)^{n+1}$ as indicated in relation (17b). In our case, for a VM97-30 magnetic steel sheet, we obtained $8.4 \cdot 10^{-3} \le \le (\rho_0/2\rho_e)^{n+1} \le 3.9 \cdot 10^{-2}$, and for a ST37-2 steel sheet $5.7 \cdot 10^{-3} \le \le (\rho_0/2\rho_e)^{n+1} \le 1.12 \cdot 10^{-2}$. Using these values and those from (8) and (17b), and knowing other parameters of the latter relation, we obtain the relative elastic energy contribution compared to the plastic one, which is equal to 3.77% for a VM97-30 magnetic steel sheet and 1.6% for a ST37-2 steel sheet. These values allow the elastic energy contribution to the energy balance given by (17a) to be neglected, and thus, relation (3) takes the form

$$Pdx = \frac{\Gamma_e B dx}{2} + \frac{\sigma_0 W B^{n+2}}{(n+1)(n+2)} \left(\frac{1}{\rho_0}\right)^{n+1} dx. \tag{18}$$

Finally, the last equation is reduced to

$$\frac{P}{B} = \frac{\Gamma_e}{2} + \frac{\sigma_0 W}{(n+1)(n+2)} \left(\frac{B}{\rho_0} \right)^{n+1}. \qquad (19)$$

With the use of (19), Mai and Cotterell [5] have shown the possibility to determine the essential work of fracture Γ_e by extrapolating the linear relationship between the tearing force per unit thickness P/B and the width of the specimen leg W.

Materials Studied. The tests are conducted on three different steel sheets. A sheet of cutting steel ST37-2 of thickness $B = 1$ and 1.5 mm used in electrical engine manufacturing and a sheet of magnetic steel VM97-30 of thickness $B = 0.3$ mm used for electric engine air-gap section. These steels are referenced with respect to the DIN standard (Table 1).

For our tests, specimens are cut in the material rolling direction. Mechanical properties of the materials, namely, yield strength R_e, ultimate strength R_m, elongation A (in %), dynamic flow stress $R_{0,d}$, and the values of σ_0 and n, which characterize the power law, are presented in Table 2.

Table 1

Chemical Composition (in %) of Investigated Steels

Type of steel sheets	Chemical compounds							
	C	Si	Mn	P	S	Cr	Ni	N
VM97-30	0.014	3.2	0.06	–	0.02	0.061	0.1	–
ST37-2	max 0.19	–	–	max 0.05	max 0.66	–	–	max 0.008

Table 2

Mechanical Properties of Investigated Steels

Type of steel sheets	Mechanical properties					
	R_e, MPa	R_m, MPa	A, %	n	σ_0, MPa	$R_{0,d}$, MPa
ST37-2	210	324	28.30	0.23	310	524
VM97-30	292	313	10.80	0.11	271	–

Experimental Results and Analysis. The tearing force per unit thickness P/B is plotted as a function of the width W (Fig. 2), and the essential work of fracture for different steel sheets is determined by extrapolating the linear curves. The values of Γ_e are equal to 853, 1866, and 620 kJ/m^2 for the steel sheet ST37-2 with $B = 1$ mm, ST37-2 with $B = 1.5$ mm, and the magnetic steel sheet VM97-30 with $B = 0.3$ mm, respectively.

These results confirm the previous conclusion [5] concerning the dependence of the essential work of fracture Γ_e on the thickness. The test results for a ST37-2 thin steel sheet of different thickness ($B = 1$ and 1.5 mm), showed that the values of Γ_e increase with thickness. This confirms the nonintrinsic character of the essential work of fracture Γ_e. The latter can be considered as a mechanical

characteristic of a thin steel sheet only for a single value of the thickness. Moreover, it is noteworthy that the tear per unit thickness P/B increases with W as long as the specimen width W does not exceed 30 mm. Upon reaching this limit, a decrease in P/B is noticed, which makes us think that the approximation of the linear behavior is no longer valid within the whole domain W studied.

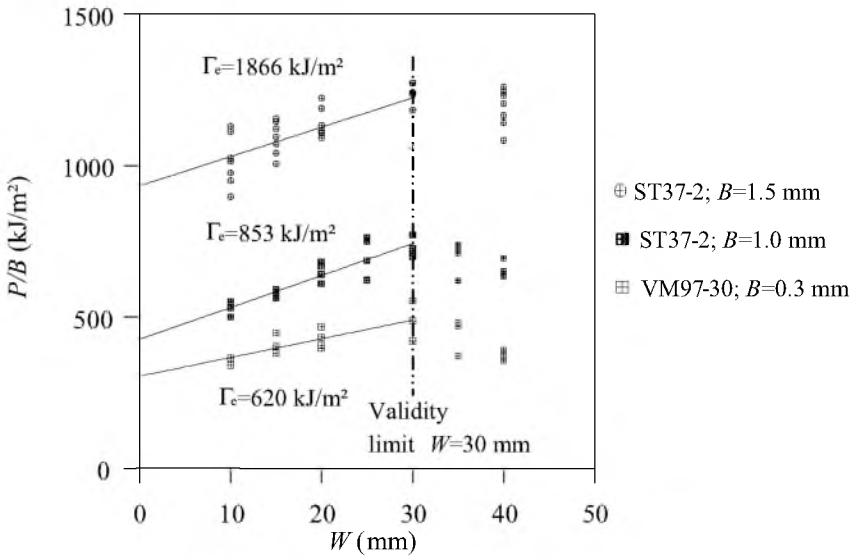

Fig. 2. The tearing force per unit thickness, P/B, versus leg width, W.

In accordance with Muscat-Fenech and Atkins [6], ρ increases with W (Fig. 3), and manifests itself in a linear growth according to the following relation:

$$\rho = \beta W + \alpha, \tag{20}$$

where β and α are constants whose values for each material tested are presented in Table 3.

The introduction of the linear relationship $\rho = \beta W + \alpha$ in Eq. (19), assuming $1/\rho \approx 1/\rho_0$, makes it possible to formulate the so-called *Corrected Mai–Cotterell* (CMC) relation in the form:

$$\frac{P}{B} = \frac{\Gamma_e}{2} + \frac{\sigma_0 B^{n+1}}{(n+1)(n+2)} \frac{W}{(\beta W + \alpha)^{n+1}}. \tag{21}$$

In this model, Γ_e is evaluated using the force value obtained during the test and the corresponding radius of curvature and leg width. Expression (21) shows that the variation of P/B according to W is not linear any more. Comparison of the Γ_e values with the use of the two models [MC model (Eq. 19) and CMC model (Eq. 21)] proposed in this study is presented in Table. 4. With regard to the scattering of experimental data on the P/B vs W relation (Fig. 2), we supplemented Γ_e calculated according to the CMC model (Eq. 21) with a

Table 3

Constants α and β

Type of steel sheets	B, mm	β	α
ST37-2	1.0	0.22	7.32
VM97-30	0.3	0.28	0.39

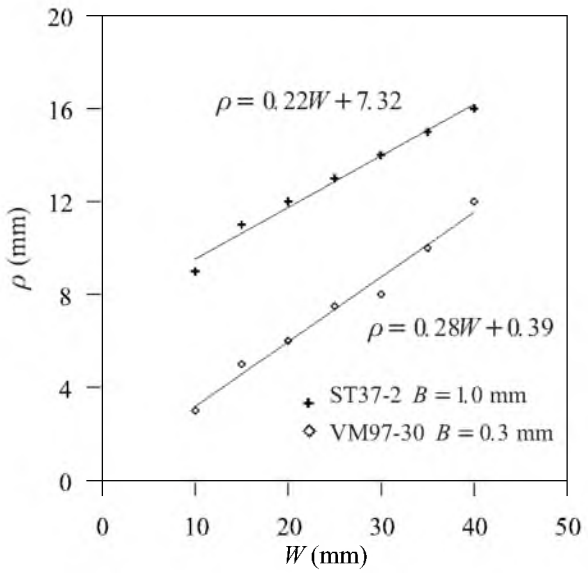

Fig. 3. The radius of curvature ρ as a function of the leg width W.

statistical analysis from which we determined the standard deviation and the confidence interval at 95% of the average Γ_e (Table 4). The results presented in Table 4 show that:

1. High values of the standard deviation confirm a large scattering of the experimental data on the P/B vs W relation (see Fig. 2).

2. The confidence interval at 95% shows that the Γ_e value determined in this sample analysis is a good estimation of the average Γ_e value in the CMC model for each material tested.

3. The value of Γ_e^{av} determined by the CMC method as compared to the reference value determined by the MC model [see respective Δ (%)], is high for ST37 steel and very close in the case of VM97 steel. This variation is probably due to the nature of the materials used in our tests, particularly, the coupling influence of $\rho(W)$ and the work hardening exponent n, which appears in the power form in the CMC model (Eq. 21).

Effect of the Loading Rate on the Essential Work of Fracture. Tests are conducted on trousers tearing test specimen (ST37-2; $B = 1.5$ mm) with the loading rate V varying between 1 and 300 mm/min. Four values are tested in this range. The essential work of fracture Γ_e is determined by the MC model (Eq. 19) for each value of V. It is obtained by extrapolating the linear relationship between the tearing force per unit thickness P/B and the width of the specimen leg W for a zero leg width (Fig. 4).

Table 4

Comparative Table of Γ_e Values

ST37-2; $B = 1$ mm			VM97-30; $B = 0.3$ mm		
Γ_e (kJ/m^2) according to MC model	Γ_e (kJ/m^2) according to CMC model	Relative error Δ (%)	Γ_e (kJ/m^2) according to MC model	Γ_e (kJ/m^2) according to CMC model	Relative error Δ (%)
853	1156 (average)	35	620	622 (average)	0.32
	$SD = 132$ $CI_{95\%} = 50$			$SD = 110$ $CI_{95\%} = 50$	

Note: Relative error $\Delta = \dfrac{\Gamma_{e,\mathrm{MC}} - \Gamma_{e,\mathrm{CMC}}}{\Gamma_{e,\mathrm{MC}}}$.

Table 5

The Essential Work of Fracture Γ_e for Different Loading Rates

V, mm/min	1	10	30	300
Γ_e, kJ/m^2	1866	1847	1843	1812

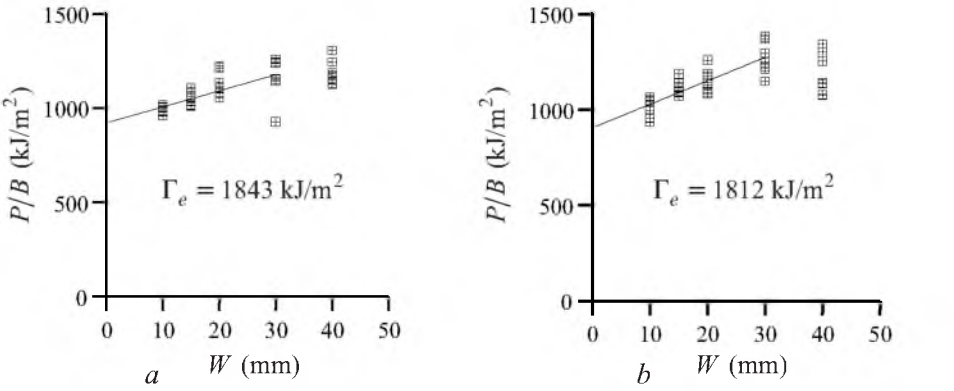

Fig. 4. Essential work of fracture Γ_e for different loading rates (ST37-2 steel, $B = 1.5$ mm): (*a*) $V = 30$ mm/min; (*b*) $V = 300$ mm/min.

A slight decrease in Γ_e (-3%) is observed when the loading rate V varies between 1 and 300 mm/min (Table 5). The magnitude of V seems to have a little effect on the values of Γ_e. Such insensitivity is in accordance with Eq. (19) in which V does not appear.

Dynamic Tearing Tests.

For dynamic tearing tests, three-leg trousers specimens are used, in which the middle leg is provided for a ring (Fig. 5a and b). These tests are performed on a Charpy test apparatus in which the hammer is replaced by a hook to seize the ring. In these dynamic tearing tests, the only variable parameter is the ligament length b (Fig. 6a), whereas the leg width is kept constant in all tests. The similarity that exists between the fracture process of dynamic tests and petalling of thin metallic sheets allows us to evaluate the material toughness according to the formulations of Landkroft and Goldsmith [7] and Kawano et al. [8].

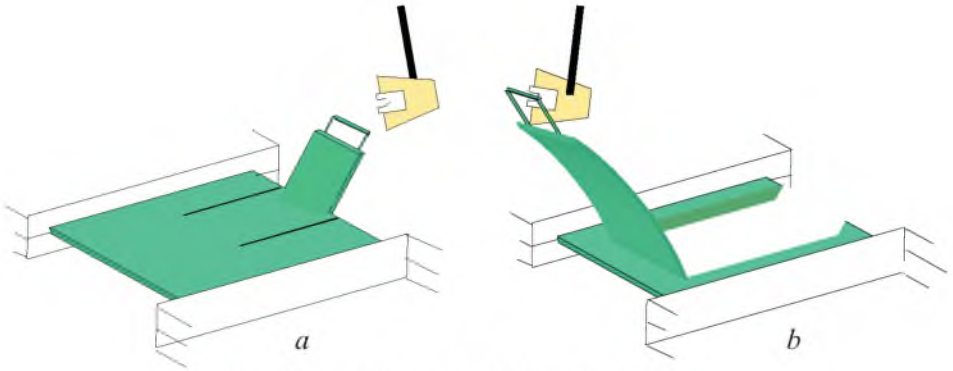

Fig. 5. Schematic illustration of the dynamic test progress.

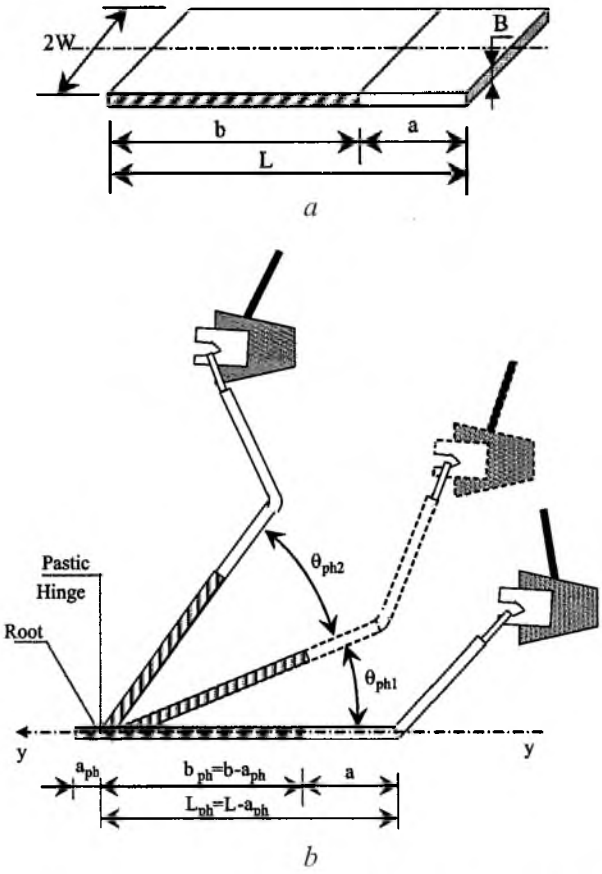

Fig. 6. Geometry of the middle leg: (a) before the test; (b) after the test.

Evaluation of the Energy Absorbed in Bending of the Middle Leg. As shown in Fig. 5b, petal formation results from bending of the specimen middle leg due to the pressure of the hook. Assuming the Landkroft and Goldsmith study [7], analysis of this process should be based on the following assumptions:

1. The force exerted by the hook is always applied at the tip of the middle leg in the normal direction to the plate.

2. Geometrical effects due to large deformation are neglected.

3. The material is regarded as rigid perfectly plastic so that no deformation occurs when the bending moment at the middle leg cross section is smaller than the plastic moment M_p and infinite large strain can occur when it exceeds M_p.

4. Only the plastic moment is taken into account in the energy balance.

5. The crack propagation rate is assumed to be always higher than the plastic hinge velocity.

Since bending of the middle leg is initiated at the moment of impact and growth in length L with outward crack propagation, it may be assumed that at each stage of the hook motion, one deals with a cantilever beam of constant thickness and rectangular shape. The fixed end of this beam moves outward with crack propagation. The situation is described in Fig. 6b. There are two stages in the absorption process. During the outward crack propagation, there will be parallel outward motion of the plastic hinge in the middle leg until the hinge arrives subsequently at this "built-in" end (the root of the middle leg). At the end of this phase, the middle leg experiences rotation θ_{ph1}. After the first stage, the moving hook and the middle leg possess kinetic energy; therefore, additional motion will take place. In this case, the plastic hinge is fixed at the root by the magnitude of the angle θ_{ph2}, which is sufficient to ensure free passage of the hook. At the end of this second stage, the middle leg may have some residual kinetic energy, especially in the case of thin plates. In this case, the rotation of the middle leg exceeds θ_{ph2} and it is detached completely from the test specimen.

The energy absorbed at the first stage of deformation is calculated. The solution of this problem was presented by Landkroft and Goldsmith [7]. Calculations were made for a triangular cantilever beam. This approach is followed here. The middle leg is modeled by a rectangular cantilever beam of constant thickness B and length L (Fig. 6a). The variable plastic moment of this geometry is given by

$$dM_p = R_e \frac{2WB^2}{4} \frac{db}{L_{ph}}. \tag{22}$$

The pure plastic moment is

$$M_p = R_e \frac{2WB^2}{4} \frac{b_{ph}}{L_{ph}}. \tag{23}$$

Here $2W$ is the width of the middle leg, a is the crack length, L is the initial lateral dimension of the specimen (as illustrated by Fig. 6a), while b_{ph} and L_{ph} are the distance of the plastic hinge travel and the length of the middle leg after the second stage, respectively (Fig. 6b). The parameter a_{ph} appearing in Fig. 6b is the distance between the root and the free edge of the leg. From experimental observations, it is found to be equal to 6.7 mm. At the second stage of motion, a rigid-body rotation of the middle leg at the fixed end takes place. The energy balance for this stage is given by

$$U = M_p \theta_{ph2} = \frac{m}{2}(v_i^2 - v_f^2) + \Delta W_R, \tag{24}$$

where v_i and v_f are the initial and the final velocity of the hook, respectively, m is the striking mass, and ΔW_R is the change in the rotational energy of the middle leg during the second stage of motion. Scibetta et al. [9] assumed that J-integral can be interpreted as the energy-rate release per unit crack area:

$$J = \frac{1}{2B} \frac{\partial U}{\partial b}\bigg|_{\theta_p} \tag{25}$$

with

$$dU = \theta_{ph2} dM_{p.} \tag{26}$$

For the practical evaluation of the J-integral, Akourri et al. [10] assume that the fracture toughness is proportional to the work spent on fracture per unit ligament area, and η-factor is introduced in the J-integral formulation:

$$J = \eta \frac{U}{2Bb_{ph}}. \tag{27}$$

For a rigid perfectly plastic material, it is easy to establish the η-factor as a function of the plastic moment. The combination of Eqs. (25) and (27) yields

$$\eta = \frac{\partial U}{\partial b} \frac{b_{ph}}{U}. \tag{28}$$

Combination of Eqs. (24), (26), and (28) gives

$$\eta = \frac{\partial M_p}{\partial b} \frac{b_{ph}}{M_p}. \tag{29}$$

The introduction of relations (22) and (23) in Eq. (29) permits us to obtain the value of the η-factor:

$$\eta = 1. \tag{30}$$

Therefore, Eq. (27) takes the form

$$J = \frac{U}{2Bb_{ph}}. \tag{31}$$

The absorbed energy is evaluated by Kawano et al. [8] in the following manner. Generally, a typical J-integral resistance ($J - R$) curve can be given as shown in Fig. 7. In region *1*, a crack initiates when the J-value reaches a certain

characteristic value for the material, J_0. This is followed by region *2*, where the gradient of the $J-R$ curve, dJ/da, decreases with the crack growth, but the crack extension is small. Then dJ/da reaches an approximately constant value in region *3*. Since the crack is not short in this study, it is assumed that the *J*-integral value can be expressed by the dotted line in Fig. 7. Using the definition of the tearing modulus [9]

$$T = \frac{E}{R_0^2}\frac{dJ}{da}, \tag{32}$$

this function can be written as follows:

$$J = \frac{1}{2B}\frac{dU}{da} = J_0 + \frac{R_0^2}{E}Ta, \tag{33}$$

where R_0 is the flow stress and J_0 is the material toughness at the initiation of fracture. Hence, if we identify the first term of Eq. (31) with relation (33), we can write

$$J = \frac{U}{2Bb_{ph}} = J_0 + \frac{R_0^2}{E}Ta. \tag{34}$$

For our dynamic tearing tests, relation (34) is rewritten as

$$J = \frac{U}{2Bb_{ph}} = J_{0,d} + \frac{R_{0,d}^2}{E}T_d a, \tag{35}$$

where $R_{0,d}$ is the dynamic flow stress, $J_{0,d}$ is the dynamic toughness at initiation, and T_d is the dynamic tearing modulus.

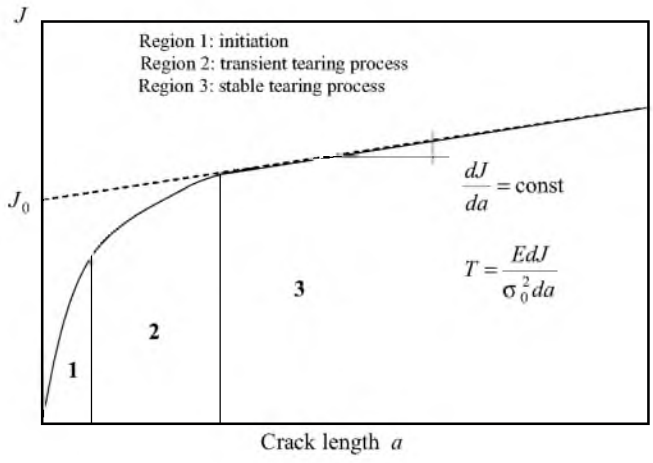

Fig. 7. Schematic illustration of a typical *J*-resistance curve.

Table 6

Geometry of the Dynamic Specimens

a, mm	5	10	15	20	25	30	35
a/L	0.08	0.15	0.23	0.31	0.38	0.46	0.54

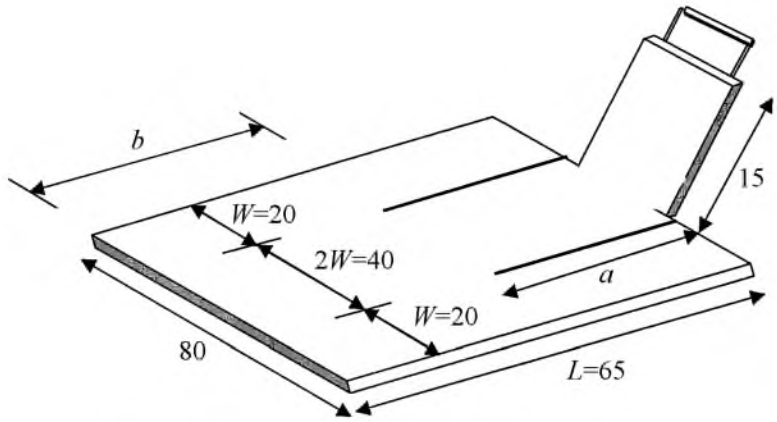

Fig. 8. A dynamic trousers-test specimen. Three-leg geometry.

Test Specimens. Specimens are cut in the rolling direction of the material and tests are conducted on ST37-2 steel sheets with thickness $B = 1.5$ mm. The specimen geometry and dimensions are given in Fig. 8. Various values of the crack length a and ratio a/L used during the tests are presented in Table 6.

Experimental Results and Analysis. The tests allow the measurement of the absorbed energy U for tearing initiation and propagation for each value of the crack length a (Fig. 9a). The value of the dynamic toughness at initiation $J_{0,d}$ is obtained from the straight-line relationship between the absorbed energy per unit area $J = U/(2b_{ph}B)$ and the crack length a by extrapolation to zero crack length (Fig. 9b), where $J_{0,d} = 1443$ kJ/m^2 and $T_d = 30$.

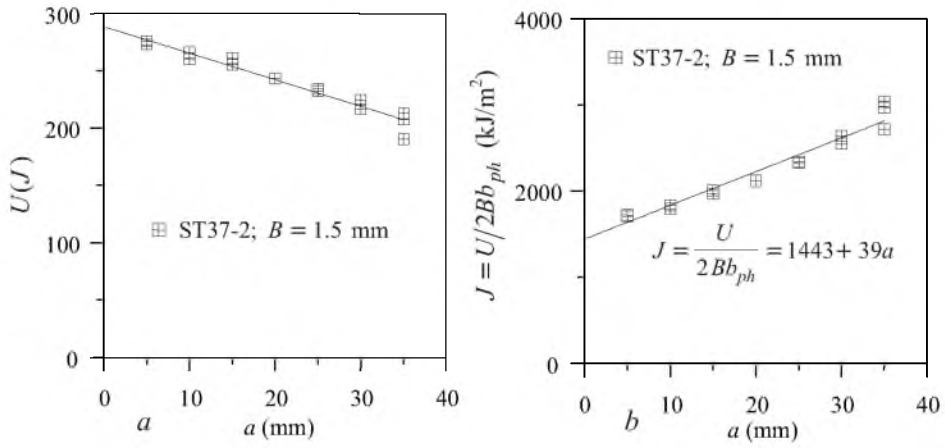

Fig. 9. Absorbed energy, U, and specific absorbed energy, J, vs various crack lengths, a.

T a b l e 7

Γ_e **and** $J_{0,d}$

Type of steel sheets	B, mm	Toughness (kJ/m^2)	
ST37-2	1.5	Static (V = 1 and 300 mm/min)	Dynamic ($V = 3\cdot10^5$ mm/min)
		$\Gamma_e^{av} = 1842$	$J_{0,d} = 1443$

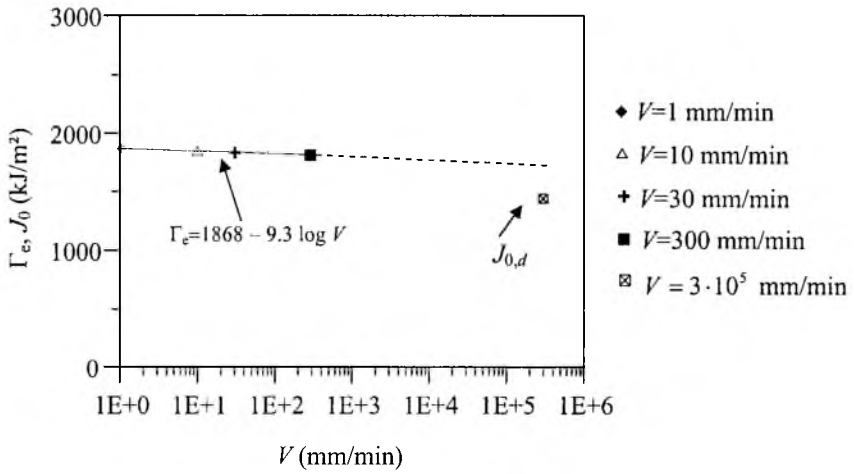

Fig. 10. The values of Γ_e and $J_{0,d}$ versus the loading rate V.

The values of Γ_e and $J_{0,d}$ characterize fracture initiation toughness at static and dynamic tearing, respectively. We compared the values of Γ_e and $J_{0,d}$. Different values of Γ_e and $J_{0,d}$ are shown in Fig. 10 and tabulated in Table 7. All these results revealed the following:

1. When the quasi-static loading rate increases (from 1 to 300 mm/min), the Γ_e and V relations are linear, and the relationship that relates Γ_e and V is as follows:

$$\Gamma_e = 1868 - 9.3 \log V. \tag{36}$$

2. When the loading rate is increased by a factor of one thousand (1000) to $3\cdot10^5$ mm/min, no significant variation of the fracture initiation toughness value occurs as shown by the $J_{0,d}$ and Γ_e ratio:

$$r_1 = \frac{J_{0,d}}{\Gamma_e} = 0.78. \tag{37}$$

For comparison, let us consider the Golovechkin and Touzlokova [12] ratio obtained in mode I fracture on aluminum and titanium alloys and on thin steel sheets:

$$r_2 = \frac{K_{\mathrm{Ic},d}^2}{K_{\mathrm{Ic},st}^2} = 0.36, \tag{38}$$

where $K_{\mathrm{Ic},d}$ and $K_{\mathrm{Ic},st}$ are the dynamic and static mode I stress intensity factors, respectively.

Comparison between the r_1 and r_2 values can be modeled according to the relationship $K_c^2 = EJ_{\mathrm{Ic}}$. We notice that for our study, the ratio between the dynamic and the static values of toughness is higher than that obtained according to Golovechkin and Touzlokova [12], which indicates that the fracture toughness of thin sheet metal in mode I fracture is more sensitive to the dynamic loading effects.

Conclusions. We have shown that when the elastic contribution is negligibly small compared to the plastic one, the tearing force P/B is related to the width W of the specimen leg by a linear relationship. The experimental data are found to be in agreement with the above behavior, provided W does not exceed 30 mm. For large values of W, such an approximation of the linear behavior is no longer valid. The radius of curvature ρ increases with W indicating that the second term in Eqs. (19) and (20), which describes the crack propagation share in the tearing process, is not negligible, its value depends on the nature of materials used. For highly ductile materials such as ST37-2 steel, its influence is more significant. Moreover, the experiments also show that Γ_e increases with the thickness B. For several loading rates V varying from 1 to 300 mm/min, the experiments indicate that Γ_e is not affected by V, while Γ_e remains constant up to the value of V 300 mm/min. In the second part of this work, dynamic tests are performed on a Charpy-test apparatus. Dynamic toughness at initiation, $J_{0,d}$, is determined. The relation between this parameter and Γ_e is calculated, which shows a slight decay of $J_{0,d}$ in relation to Γ_e. It seems that in the case of mode III tearing of a thin steel sheet, the toughness is relatively insensitive to the loading rate.

Резюме

Представлено енергетичний аналіз статичного руйнування тонких стальних листів за типом K_{III}. При динамічних випробуваннях використовувалось обладнання для зразків типу Шарпі. Статичні випробування трьох видів стальних дисків на розрив свідчать, що лінійне співвідношення Мая–Коттрелла справедливе для зразків із шириною робочої частини до 30 мм. У такому діапазоні питома робота руйнування Γ_e визначається у відповідності з моделлю Мая–Коттрелла. Досліджувалась кінетика Γ_e в залежності від товщини листа B, радіуса кривини ρ і швидкості навантаження V. Удосконалена модель включає співвідношення ρ/W. Окрім того, змінюючи швидкість навантаження V від 1 до 300 мм/хв, встановлено, що питома робота руйнування Γ_e не залежить від неї. Показано незначне зменшення динамічної тріщиностійкості $J_{0,d}$.

1. B. Cotterell and J. K Reddel, "The essential work of plane stress ductile fracture," *Int. J. Fract.*, **13**, 267–277 (1977).
2. K. B. Broberg, "Crack-growth criteria and nonlinear fracture mechanism," *J. Mech. Phys. Solids*, **19**, 407–418 (1971).

3. G. Pluvinage, *Mécanique Élastoplastique de la Rupture*, Edition Cépadues Toulouse (1989), pp. 139–153.
4. J. P. Keustemans, *Analyse Fractale et Mécanique de la Rupture*, Thèse de Doctorat de l'Universite Catholique de Louvain (1995), Ch. VI, pp. 6–7.
5. Y. W. Mai and B. Cotterell, "The essential work for tearing of ductile metals," *Int. J. Fract.*, **24**, 229–318 (1984).
6. C. M. Muscat-Fenech and A. G. Atkins, "Elastoplastic trouser tear testing of sheet materials," *Int. J. Fract.*, **67**, 69–80 (1994).
7. B. Landkroft and W. Goldsmith, "Petalling of thin metallic plates during penetration by cylindro-conical projectiles," *Int. J. Solids Struct.*, **21**, No. 3, 245–266 (1985).
8. S. Kawano, E. Kaminishi, M. Yamashita, and S. Shimizu, "Energy-absorbing of ductile thin metal sheet under quasi-static penetration by conical punch," *Int. JSME*, Serie 1, **31**, No. 1, 108–116 (1988).
9. M. Scibetta, R. Chaouadi, and E. van Walle, "Fracture toughness analysis of circumferentially-cracked round bars," *Int. J. Fract.*, **104**, 145–168 (2000).
10. O. Akourri, M. Louah, A. Kifani, et al., "The effect of notch radius on fracture toughness J_{Ic}," *Eng. Fract. Mech.*, **65**, 491–505 (2000).
11. P. C. Paris, Z. Tada, A. Zahoor, and H. Ernst, "The theory of the tearing mode of elastic-plastic crack growth," in: *ASTM STP 668* (1978), pp. 5–6.
12. Y. N. Golovechkin and N. I. Touzlokova, *Buckling Stability of Ship Hull* [in Russian], Sudostroenie, Moscow (1993), pp. 104–115.

Received 29. 12. 2002